Measurement of $E2$-$E0$ strength in the isovector giant resonance (GQR-GMR) region of ^{28}Si nuclei through the $(e, e'n)$ reaction

K. Kino,* T. Saito,† T. Nakagawa,‡ T. Tamae, I. Nishikawa, Y. Asano,§ H. Toda,‖ and M. Watabe
Laboratory of Nuclear Science, Tohoku University, Mikamine, Taihaku-ku, Sendai 982-0826, Japan

T. Nakagawa,¶ H. Tsubota, K. Takahashi,** and M. Utoyama
Department of Physics, Graduate School of Science, Tohoku University, Aramaki, Aoba-ku, Sendai 980-8578, Japan

M. Higuchi and Y. Matsuura††
Faculty of Engineering, Tohoku Gakuin University, Chuo, Tagajo 985-8537, Japan

H. Ueno¶ and T. Suzuki‡‡
Department of Physics, Yamagata University, Kojirakawa, Yamagata 990-8560, Japan
(Received 1 December 2005; published 28 March 2006)

We have measured the ^{28}Si$(e, e'n)$ reaction in the excitation energy range 21.5–40.5 MeV at three effective momentum transfers, 0.38, 0.49, and 0.60 fm^{-1}. The $E1$ and $E2$-$E0$ components were separated based on their different momentum-transfer dependences. The $E1$ strength obtained was found to agree with that of photoreactions in shape and strength. The strength of the $E2$-$E0$ component at low excitation energies was very small when compared with that of the $(e, e'p)$ reaction. At higher excitation energies, the $E2$-$E0$ component has a bump structure at about 26–30 MeV and it is suggested that it has an isovector character by comparison with (α, α') reaction data. This is supported by results of a ^{28}Si(^{7}Li,^{7}Be)^{28}Al experiment. The $E2$-$E0$ strength of 37.9(±4.7)% in the isovector $E2$ energy-weighted sum rule is exhausted in the excitation energy range 22.5–40.5 MeV.

DOI: 10.1103/PhysRevC.73.034614 PACS number(s): 25.30.Dh, 24.30.Cz, 27.30.+t

I. INTRODUCTION

The giant resonance is a fundamental manifestation of the collective motion of nucleons in a nucleus and is characterized by a variety of oscillation modes that can be classified by three quantum numbers, multipolarity (L), isospin (T), and spin (S). In this paper, we study the electric isovector giant monopole and quadrupole resonances (IVGMR, IVGQR), which are represented by transitions with $\Delta L = 0$ and 2, respectively, satisfying both $\Delta T = 1$ and $\Delta S = 0$. Although these are basic modes, experimental data for them are still scarce for light nuclei. The restoring force for these vibration modes depends on the isospin symmetry-energy; in heavy nuclei, the contribution of the symmetry-energy in the nuclear volume dominates, whereas the surface effect is expected to be important in light nuclei [1]. Hence the systematics of the excitation energy is dependent on nuclear mass, and experimental data of the energy for light to heavy nuclei is desired to help better understand the IVGMR and IVGQR.

The IVGMR has been observed through the $(\pi^{\pm}, \pi^{0})$ [2], (n, p) [3], (^{13}C,^{13}Nn) [4], (^{7}Li,^{7}Be) [5,6], and (^{3}He,tp) [7] reactions. The IVGQR has been studied by electron scattering [8] and photoreactions [9]. The systematics of the excitation energies accumulated from experimental data in medium-heavy to heavy nuclei are $59.2A^{-1/6}$ and $130A^{-1/3}$ MeV for the IVGMR and IVGQR, respectively [10]. These give excitation energies of 34 and 43 MeV for the IVGMR and IVGQR in ^{28}Si. These energies are about 13 and 24 MeV higher than the experimentally obtained centroid energies of the isoscalar giant monopole and quadrupole resonances (ISGMR, ISGQR) [11] with $\Delta T = 0$.

In this paper, we report experimental results for the $E2$-$E0$ strength distribution in ^{28}Si obtained by the $(e, e'n)$ reaction, which may contain IVGQR and/or IVGMR components. For ^{28}Si$(e, e'p)$ experiments [12], a larger $E2$-$E0$ strength than that for the $(\alpha, \alpha'p)$ reaction has been reported for the excitation energy region from 14 to 22 MeV. In this energy region, both the ISGMR and ISGQR are believed to exist and the excessive strength in the $(e, e'p)$ reaction was interpreted

*Present address: Center for Nuclear Study, University of Tokyo, 2-1 Hirosawa, Wako, Saitama 351-0198, Japan.
†Present address: Faculty of Engineering, Tohoku Gakuin University, Chuo, Tagajo 985-8537, Japan.
‡Present address: Toshiba Co., Shinsugitacho, Isogo-ku, Yokohama 235-8523, Japan.
§Present address: Catena Co., Shiomi, Koto-ku, Tokyo 135-8565, Japan.
‖Present address: Toshiba Co., Toshibacho, Fuchu 183-0043, Japan.
¶Present address: Tohoku Institute of Technology, Kasumicho, Taihaku-ku, Sendai 982-8577, Japan.
**Present address: Art Kagaku Co., Muramatsu, Tokai, Ibaraki 3129-40, Japan.
††Present address: Aza-Higashinoda 67, Medeshimashiote, Natori 981-1238, Japan.
‡‡Present address: Department of Physics, Graduate School of Science, Tohoku University, Aramaki, Aoba-ku, Sendai 980-8578, Japan.

as being due to the IVGQR and/or IVGMR. This may suggest large overlaps of the isoscalar and isovector excitations of the GMR and/or GQR in ^{28}Si nuclei. However, the experiments were performed for a limited range of excitation energy and the whole structures of the IVGMR and IVGQR were not explored. On the other hand, it has been suggested that the IVGQR and IVGMR appear at 27 and 31 MeV with widths of 3.5 and 4.0 MeV, respectively, in the ^{28}Si(^{7}Li,^{7}Be)^{28}Al reaction [5]. These widths are too narrow to have strengths in the ISGMR and ISGQR region for ^{28}Si$(e, e'p)$ [12]. Both the experimental data for the IVGMR from the $(\pi^{\pm}, \pi^{0})$ reaction and those for the IVGQR from electron scattering and photoreactions show a trend of increasing width of the resonances as the mass number decreases from heavy to medium-heavy nuclei. In medium-heavy nuclei, a recent ^{60}Ni(^{7}Li,^{7}Be)^{60}Co experiment [6] shows a width of 10 MeV in ^{60}Co for the IVGMR, and electron scattering and photoreaction experiments [8,9] have shown widths of 10–15 MeV for the IVGQR in ^{40}Ca. These results suggest that the widths of the IVGMR and IVGQR in ^{28}Si are wider than 10 and 10–15 MeV, respectively.

The contribution of the direct-knockout process has been extracted for the ^{16}O$(e, e'p_0)$ reaction data [13], which was taken at a momentum transfer similar to that of the present paper. It is suggested that this process increases from an excitation energy of 22 MeV in ^{16}O, which is close to the energy of the ISGQR peak in ^{28}Si. Therefore the direct-knockout process may interfere with the observation of the IVGMR and/or IVGQR, which are located at higher energies than the ISGQR. Neutron coincidence measurements under the present electron scattering conditions, in which the longitudinal component of virtual photons is dominant, could give a lower contribution from the direct-knockout process compared with the $(e, e'p)$ reaction.

II. EXPERIMENT

Measurements were performed using 150- and 198-MeV continuous electron beams from the Stretcher Booster Ring at the Laboratory of Nuclear Science (LNS) of Tohoku University. The duty factor and beam current were 80–90% and 150–300 nA, respectively. A target of chemically pure silicon (92.2% ^{28}Si) with a thickness of 118.8 mg/cm^2 was used.

Scattered electrons were momentum analyzed by a double-focusing magnetic spectrometer and detected by a combination of a vertical drift chamber (VDC) in the focal plane and three layers of 5, 5, and 8-mm thick plastic scintillation counters behind the VDC. The VDC provided information on the momentum of the scattered electrons and the scintillation counters were used for fast signals of the electron arm. The spectrometer was set at a scattering angle of 28° at incident energies of 150 and 198 MeV and 35° at 198 MeV. These correspond to the effective momentum transfers [14] $q_{\rm eff}$ of 0.38, 0.49, and 0.60 fm^{-1}, respectively, and are similar to the values in the ^{28}Si$(e, e'p)$ experiment [12]. The excitation energy range was from 21.5 to 40.5 MeV.

Emitted neutrons were detected using eight neutron detectors, which were placed at 58°, 83°, 108°, 133°, 158°, 213°, 238°, and 263° to the electron beam direction. These were placed in the plane defined by the incident electron beam and detected scattered electrons. Each detector consisted of NE213 liquid scintillator in an aluminum cylindrical vessel of 103 × 180 mm ϕ and a 5-in. photomultiplier tube. The detectors were placed 0.85 m from the target and the neutron energy was determined by the time-of-flight method. The detectors were shielded by concrete, paraffin, and lead from the huge number of γ rays and neutrons in the experimental hall. Plates of ^{209}Bi with a thickness of 4 or 6 cm were placed in front of the detectors to absorb scattered electrons and γ rays from the target. In order to remove remaining γ-ray events in the offline analysis, we made two measurements of the signals from the neutron detectors; one used pulse shape discriminator modules and the other used the charge comparison method. The detection threshold for neutrons was set to 1.7 MeV and the detection efficiency was determined by a combination of the code TOTEFF [15] and experimental data using a ^{252}Cf neutron source near the detection threshold. The data were obtained using the data acquisition system "NewKoala" [16], which has been newly developed for high counting-rate $(e, e'X)$ experiments at LNS.

III. ANALYSIS AND DISCUSSION

A. Missing energy spectra

Figure 1 shows the missing energy spectra at certain excitation energies for the ^{28}Si$(e, e'n)^{27}$Si reaction. Neutrons populate two main groups of the ^{27}Si levels. The first group is near the ^{27}Si ground state: n_0 (17.18 MeV), n_1 (17.96 MeV), and n_2 (18.14 MeV). The other group is at higher missing energies, from n_3 (19.34 MeV) to about 25 MeV. In the spectrum with an excitation energy of 33.5 MeV, the latter group is distributed around about 22 MeV.

In this paper, we analyze the region of missing energy from n_0 to 25 MeV. However, only events with missing energy below $\omega - 3$ MeV were analyzed in the excitation energy from 21.5 to 27.5 MeV, to avoid large statistical uncertainties due to the low detection efficiency of the neutron detectors near the threshold. Here, ω is the excitation energy. The present analysis does not include np decay since its threshold is 24.64 MeV, which is close to the maximum missing energy in the analysis. The threshold energy of $2n$ decay is 30.49 MeV and therefore this decay channel is also excluded.

The residual states for the n_0, n_1, and n_2 decays have spin-parities of $J^{\pi} = 5/2^{+}, 1/2^{+}$, and $3/2^{+}$, respectively. They correspond naively to the states with unpaired $1d_{5/2}$, $2s_{1/2}$, and $1d_{3/2}$ shell neutrons in ^{27}Si nuclei, respectively. The strengths of n_0 and $n_{1,2}$ are comparable, although the peaks cannot be separated due to the limited missing-energy resolution. This is similar to the case of p_0 and $p_{1,2}$ in the ^{28}Si$(e, e'p)$ experiment [12]. The strength of the group in the missing energy region from n_3 to about 25 MeV is almost as great as that of $n_{0,1,2}$ at excitation energies of 28.0 MeV and higher in Fig. 1. A similar population has been observed in a quasi-free $(e, e'p)$ experiment for ^{28}Si [17]. Moreover, the angular correlations of the analyzed events exhibit forward peaked structures, as shown in Fig. 2. These results suggest that direct decay from the one-particle–one-hole state of the giant

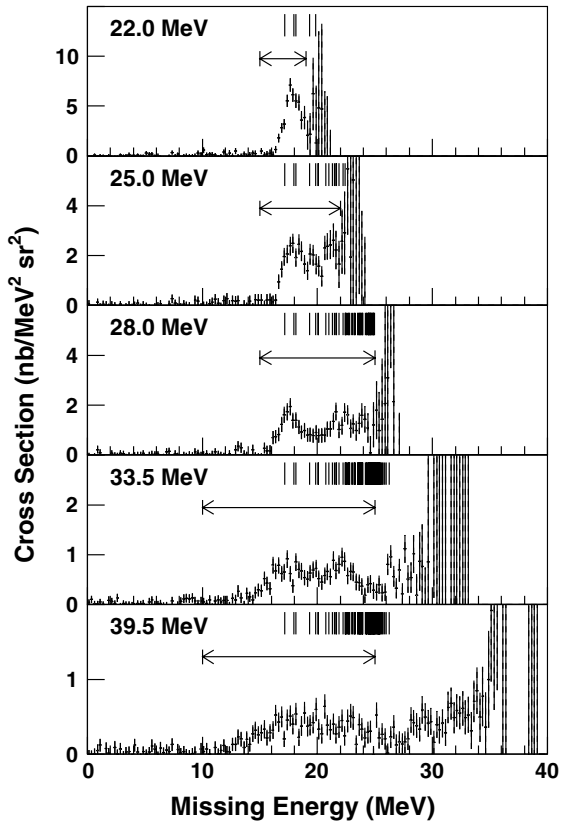

FIG. 1. Missing energy spectra for the ^{28}Si$(e, e'n)^{27}$Si reaction at $q_{\rm eff} = 0.49\,{\rm fm}^{-1}$. Shown are averaged cross sections for all the neutron detectors. The values in the figure represent excitation energies. The arrows indicate the missing energy regions that are analyzed. The lower limit of each arrow is defined so that n_0 is fully included. The short lines above each spectrum represent the energy levels of the residual nucleus ^{27}Si, containing levels corresponded to n_0(17.18 MeV) to n_{80} (26.25 MeV).

resonances dominates the ^{28}Si$(e, e'n)$ reaction, as expected for light nuclei.

B. Separation of $E1$ and $E2$-$E0$ components

As shown in Fig. 2, the angular correlations of neutrons were fitted with Legendre polynomials to obtain form factors. The following function was used with five free parameters, assuming $E0$, $E1$, and $E2$ longitudinal transitions:

$$\frac{d^3\sigma}{d\omega d\Omega_{\rm e} d\Omega_{\rm n}} = A_0\{1 + b_1 P_1(x) + b_2 P_2(x) + b_3 P_3(x) + b_4 P_4(x)\}, \quad (1)$$
$$x = \cos(\theta_{\rm n}).$$

Here, $P_1(x)$, $P_2(x)$, $P_3(x)$, and $P_4(x)$ are Legendre polynomials and A_0, b_1, b_2, b_3, and b_4 are fit parameters. The angle of the neutrons ($\theta_{\rm n}$) is taken with respect to the momentum-transfer direction. Interference of the large longitudinal transition with small transverse transition could be included in the angular correlations, which are represented by terms with associated Legendre polynomials $P_1^1(x)$, $P_2^1(x)$, $P_3^1(x)$, and $P_4^1(x)$. Among these functions, $P_1^1(x)$ and $P_3^1(x)$ can affect the parameter A_0 because the integrated values of these functions are not zero in the measured angular region. The effect of $P_3^1(x)$ was found to be negligible compared with the statistical uncertainty in the fits. In this analysis, the deviation of A_0 for fits with and without $P_1^1(x)$ was taken into account in the systematic uncertainty.

We separated the form factor $|F(q_{\rm eff}, \omega)|^2$, obtained by dividing $4\pi A_0$ by the Mott cross section, into $E1$ and $E2$-$E0$ components based on their momentum-transfer dependences. The dependences of the $E0$ and $E2$ form factors in electron scattering are too similar for them to be separated. The transverse transition was ignored in this process since the longitudinal transition dominates. In order to take into account the different kinematic factors $V_{\rm L}$ for each q and ω, the separation was performed using the form factors divided by $V_{\rm L}$, with the factor $V_{\rm L}$ defined by $((E_{\rm i} - E_{\rm f})^2 - q^2)^2/q^4$, where q is the momentum transfer and $E_{\rm i}$ and $E_{\rm f}$ are the initial and final electron energies, respectively.

The momentum-transfer dependences of the $E1$ and $E2$-$E0$ components were assumed to not be affected by the excitation

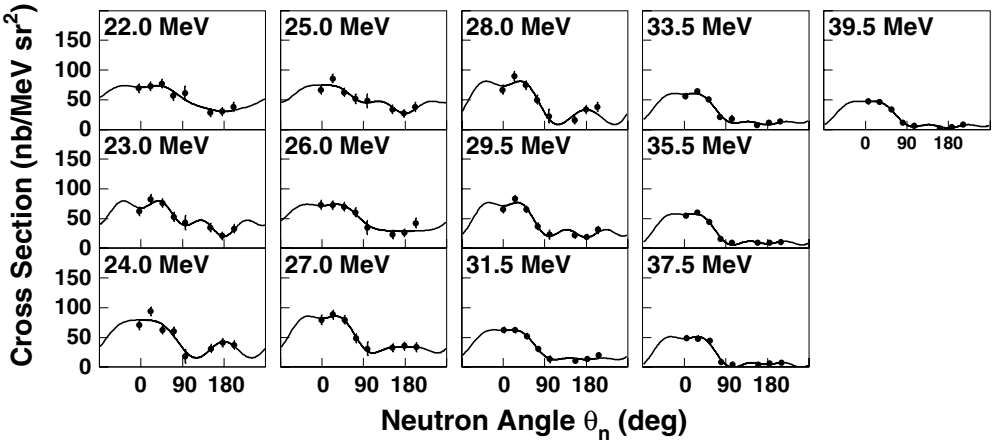

FIG. 2. Angular correlations of neutrons at $q_{\rm eff} = 0.49\,{\rm fm}^{-1}$. The excitation energy is written in each plot. The neutron angle is taken with respect to the momentum-transfer direction for electron scattering. The solid lines show Legendre-polynomial fits, as explained in the text.

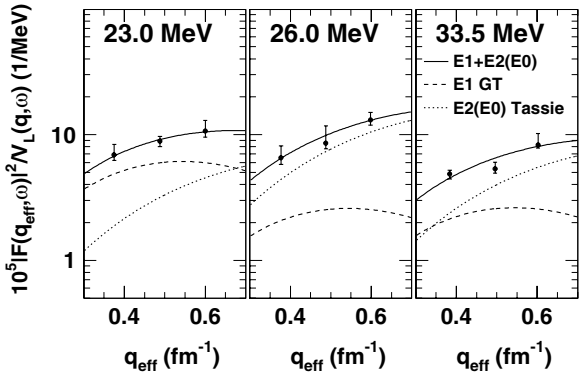

FIG. 3. Examples of $E1$ and $E2$-$E0$ separation at excitation energies of 23.0, 26.0, and 33.5 MeV. The dashed and dotted lines show form factors with respect to the effective momentum transfer, calculated by the Goldhaber-Teller [18] and Tassie [19] models, respectively. Each amplitude was determined to best fit the experimental data. The solid line is the sum of each amplitude.

energy, as shown by the following equation:

$$|F(q_{\rm eff},\omega)|^2/V_{\rm L}(q,\omega) = a_{E1}(\omega)\cdot|F_{E1}(q_{\rm eff})|^2 + a_{E2\text{-}E0}(\omega)\cdot|F_{E2\text{-}E0}(q_{\rm eff})|^2. \quad (2)$$

Here, the parameters $a_{E1}(\omega)$ and $a_{E2\text{-}E0}(\omega)$ are proportional constants of $|F_{E1}(q_{\rm eff})|^2$ and $|F_{E2\text{-}E0}(q_{\rm eff})|^2$, respectively. The functions $|F_{E1}(q_{\rm eff})|^2$ and $|F_{E2\text{-}E0}(q_{\rm eff})|^2$ represent the dependences of the $E1$ and $E2$-$E0$ form factors on the momentum transfer, where the Goldhaber-Teller [18] and Tassie [19] models were employed. In these models, the charge radius of the ground state of ^{28}Si was used as the transition charge density radius. Figure 3 shows fits using Eq. (2) at certain excitation energies. The dashed and dotted lines show the $E1$ and $E2$-$E0$ components, respectively, and the solid line represents their sum.

Figure 4 shows a comparison of the decomposed $E1$ form factor with two sets of $^{28}\mathrm{Si}(\gamma,n)+(\gamma,np)+(\gamma,2n)$ data [20,21]. The closed circles show the form factor of the present data at $q_{\rm eff} = 0.49\,\mathrm{fm}^{-1}$. For the photoreaction data, Siegert's theorem [22] was used to transform the transverse transition probability to a longitudinal transition probability at a photon point, and then the Goldhaber-Teller model [18] was employed to deduce the form factor at $q_{\rm eff} = 0.49\,\mathrm{fm}^{-1}$ from the photon point. In the figure, the diamonds and dots show the two sets of reduced photoreaction data. The above procedure is based on the assumption that the photoreaction data are dominated by the $E1$ excitation. Details of the procedure have been described in a previous paper [23]. The isovector giant dipole resonance in ^{28}Si has a peak at about 20 MeV, as shown in Fig. 4. Both form factors for the two sets of photoreaction data decrease as the excitation energy increases in the present experimental energy region. They are similar in shape and strength to the present data. Therefore, we regard the separation of the $E1$ and $E2$-$E0$ components as having been successfully performed in this analysis.

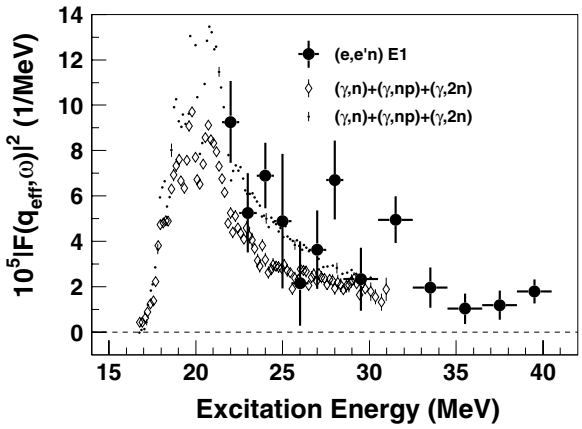

FIG. 4. Comparison of obtained $E1$ form factors at $q_{\rm eff} = 0.49$ fm^{-1} with photoreaction data. The closed circles show the present results and the diamonds and dots represent the reduced form factors of the two sets of $^{28}\mathrm{Si}(\gamma,n)+(\gamma,np)+(\gamma,2n)$ data [20,21].

C. $E2$-$E0$ component

The $E2$-$E0$ strength distributions obtained are shown in Fig. 5, together with results measured by different probes. The excitation-energy dependence of the $E2$-$E0$ form factor for the $(e,e'n)$ reaction presented in Fig. 5(a) is different from that of the $E1$ form factor shown in Fig. 4. The present $E2$-$E0$ strength has a bump structure from 26 to 30 MeV.

In Fig. 5(a), the present $E2$-$E0$ form factors are compared with measured values for $^{28}\mathrm{Si}(e,e'p)$ and $^{28}\mathrm{Si}(e,e'\alpha)$ [12], at and below the lowest measured excitation energy in the present experiment. The $(e,e'p)$ and $(e,e'\alpha)$ data include all proton and α decay channels. The $E2$-$E0$ strength of $^{28}\mathrm{Si}(e,e'p)$ increases with excitation energy up to about 17 MeV and fluctuates but remains high at 23 MeV, while that of $^{28}\mathrm{Si}(e,e'\alpha)$ decreases from 20–23 MeV. The present $E2$-$E0$ strength is suppressed compared with the $(e,e'p)$ data in which even the $p_{0,1,2}$ decay channel has a strength half that of the total $(e,e'p)$ strength.

Figure 5(b) compares the present $E2$-$E0$ strength represented by the strength in the isovector $E2$ energy-weighted sum rule (EWSR) [24] with the $E2$ and $E0$ strengths in the (α,α') reaction [11], which is sensitive to isoscalar excitations. In the figure, the strengths of the latter reaction are scaled down to allow comparison of the dependences on the excitation energy. In the excitation energy region above 22.5 MeV, the $E0$ and $E2$ strengths in (α,α') decrease gradually as the excitation energy increases. On the other hand, the $(e,e'n)$ strength increases up to about 26 MeV. This difference implies that the present $E2$-$E0$ strength contains an isovector excitation.

Figure 5(c) compares the present results with the $\Delta S = 0$ component in the $^{28}\mathrm{Si}(^7\mathrm{Li},^7\mathrm{Be})^{28}\mathrm{Al}$ reaction [5]. The contribution from the isovector giant dipole resonance is subtracted in the $^{28}\mathrm{Si}(^7\mathrm{Li},^7\mathrm{Be})^{28}\mathrm{Al}$ spectrum and therefore the isovector $E0$ and $E2$ should be the main transitions. The dashed line represents the $^{28}\mathrm{Si}(^7\mathrm{Li},^7\mathrm{Be})^{28}\mathrm{Al}$ spectrum normalized to the present data in the excitation energy region of 28.5–32.5 MeV. Both the present data and the $^{28}\mathrm{Si}(^7\mathrm{Li},^7\mathrm{Be})^{28}\mathrm{Al}$ data increase as the excitation energy increases from 24 to 30 MeV. This result supports the interpretation that the bump structure from 26 to 30 MeV for $(e,e'n)$ includes an isovector excitation, as suggested by the comparison with the (α,α') reaction in Fig. 5(b).

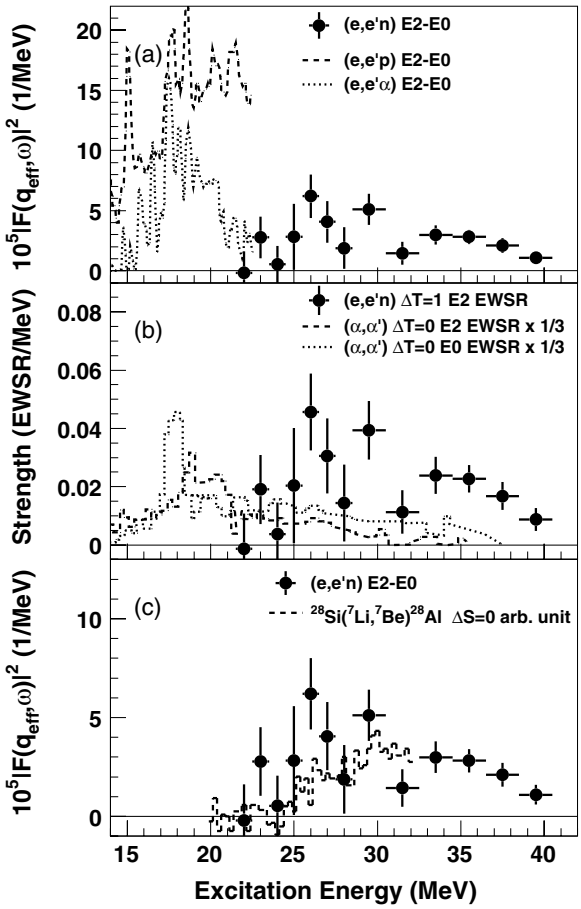

FIG. 5. Comparison of present $E2$-$E0$ form factors at $q_{\text{eff}} = 0.49$ fm^{-1} and strength of the isovector $E2$ energy-weighted sum rule with other experimental data. The closed circles show the present results. (a) Comparison with the $E2$-$E0$ form factors of the ^{28}Si$(e, e'p)$ (dashed line) and ^{28}Si$(e, e'\alpha)$ (dotted line) reaction data taken at $q = 0.49$ fm^{-1} [12]. (b) Comparison with the $E2$ (dashed line) and $E0$ (dotted line) strengths of the (α, α') reaction in the isoscalar energy-weighted sum rule [11]. An arbitrary scaling factor of 1/3 has been applied for both the dashed and dotted lines. (c) Comparison with the strength distribution of the $\Delta S = 0$ component in the ^{28}Si$(^7$Li,^{7}Be$)^{28}$Al reaction, in which the contribution from the isovector giant dipole resonance has been already subtracted [5]. The dashed line represents the ^{28}Si$(^7$Li,^{7}Be$)^{28}$Al data normalized to the present data in the excitation energy region of 28.5–32.5 MeV.

The strength for the present data shown in Fig. 5(b) is 37.9(±4.7)% of the fraction of the isovector $E2$ EWSR in the excitation energy region from 22.5 to 40.5 MeV. The strength of the isovector $E2$ EWSR from the (e, e') experiment for excitation energies of 20–30 MeV has been reported to be 10% at least and 35% at most, depending on the estimate of the background [25]. The present $E2$-$E0$ strength for excitation energies of 22.5–30.5 MeV corresponds to 21.2(±4.0)% of the isovector $E2$ EWSR and accounts for most of the (e, e') strength, even though the proton decay channels are not included. We also evaluated the fraction of the present $E2$-$E0$ strength in the summed strengths of the isovector $E0$ and $E2$ EWSRs, since the $E2$ and $E0$ components cannot be separated in the present experiment. In order to perform this evaluation in a unit of the $E2$ reduced transition probability $[B(E2)]$, the $E0$ reduced transition probability $[B(E0)]$ obtained from the $E0$ EWSR was transformed to that of $E2$ using the following relation, $dB(E2)/d\omega = 25/16\pi \cdot dB(E0)/d\omega$ [26]. The fraction was found to be 25.2(±3.1)%.

IV. CONCLUSION

We have measured the ^{28}Si$(e, e'n)$ reaction in the ^{28}Si excitation energy range 21.5–40.5 MeV and at effective momentum transfers of 0.38, 0.49, and 0.60 fm^{-1}. There are two dominant populations in the missing energy spectra. One group is near the ground state of ^{27}Si and the other is located around a missing energy of 22 MeV. Events with missing energy below $\omega - 3$ MeV in the excitation energy region from 21.5 to 27.5 MeV and events with the missing energy less than 25 MeV in the excitation energy above 27.5 MeV were analyzed.

The $E1$ and $E2$-$E0$ components show quite different shapes. The $E1$ strength decreases as the excitation energy increases and its shape and strength are largely in agreement with photoreaction data. On the other hand, the $E2$-$E0$ strength increases from 22 to 26 MeV as the excitation energy increases and has a bump structure at an excitation energy about 26–30 MeV.

The present $E2$-$E0$ data and (α, α') strength distributions differ. The former increases as the excitation energy increases above 22 MeV and the latter decrease. This result implies that the present $E2$-$E0$ strength contains an isovector excitation. This is also supported by a comparison with the ^{28}Si$(^7$Li,^{7}Be$)^{28}$Al data, which shows an isovector $E2$-$E0$ strength distribution similar to the present result. The present $E2$-$E0$ strength exhausts 37.9(±4.7)% of the isovector $E2$ energy-weighted sum rule in the excitation energy region from 22.5 to 40.5 MeV. This implies that a large fraction of the isovector monopole and/or quadrupole resonances exists, the strength of which has a bump structure from 26 to 30 MeV.

ACKNOWLEDGMENT

We would like to thank the linac crew of the Laboratory of Nuclear Science of Tohoku University for providing a quality electron beam.

[1] M. N. Harakeh and A. van der Woude, *Giant Resonances* (Clarendon Press, Oxford, 2001), p. 203, and references therein.
[2] A. Erell, J. Alster, J. Lichtenstadt, M. A. Moinester, J. D. Bowman, M. D. Cooper, F. Irom, H. S. Matis, E. Piasetzky, and U. Sennhauser, Phys. Rev. C **34**, 1822 (1986).
[3] T. D. Ford *et al.*, Phys. Lett. **B195**, 311 (1987).
[4] I. Lhenry, Nucl. Phys. **A599**, 245c (1996).
[5] S. Nakayama, T. Yamagata, M. Tanaka, M. Inoue, K. Yuasa, T. Itahashi, H. Ogata, N. Koori, K. Shima, and M. B. Greenfield, Phys. Rev. C **46**, 1667 (1992).
[6] S. Nakayama *et al.*, Phys. Rev. Lett. **83**, 690 (1999).

[7] R. G. T. Zegers, A. M. van den Berg, S. Brandenburg, M. Fujiwara, J. Guillot, M. N. Harakeh, H. Laurent, S. Y. van der Werf, A. Willis, and H. W. Wilschut, Phys. Rev. C **63**, 034613 (2001).
[8] R. Pitthan, in *Giant Multipole Resonances*, Proceedings of the Giant Multipole Resonance Topical Conference, edited by F. E. Bertrand (Harwood Academic Publishers, Chur, 1980), p. 161.
[9] D. A. Sims *et al*., Phys. Rev. C **55**, 1288 (1997).
[10] A. van der Woude, *Electric and Magnetic Giant Resonances in Nuclei* (World Scientific, Singapore, 1991), pp. 181 and 185.
[11] D. H. Youngblood, Y.-W. Lui, and H. L. Clark, Phys. Rev. C **65**, 034302 (2002).
[12] Th. Kihm, K. T. Knöpfle, H. Riedesel, P. Voruganti, H. J. Emrich, G. Fricke, R. Neuhausen, and R. K. M. Schneider, Phys. Rev. Lett. **56**, 2789 (1986).
[13] V. F. Dmitriev, D. M. Nikolenko, S. G. Popov, I. A. Rachek, D. K. Toporkov, E. P. Tsentalovich, B. B. Woitsekhowski, and V. G. Zelevinsky, Nucl. Phys. **A464**, 237 (1987).
[14] H. Überall, *Electron Scattering from Complex Nuclei* (Academic Press, New York, 1971), p. 170.
[15] R. R. Doering, D. M. Patterson, and A. Galonsky, Phys. Rev. C **12**, 378 (1975).
[16] M. Kawabata and M. Mutoh, Nucl. Instrum. Methods Phys. Res. A **454**, 460 (2000).
[17] J. Mougey, M. Bernheim, A. Bussière, A. Gillebert, Phan Xuan Ho, M. Priou, D. Royer, I. Sick, and G. J. Wagner, Nucl. Phys. **A262**, 461 (1976).
[18] M. Goldhaber and E. Teller, Phys. Rev. **74**, 1046 (1948).
[19] L. J. Tassie, Aust. J. Phys. **9**, 407 (1956).
[20] J. T. Caldwell, R. R. Harvey, R. L. Bramblett, and S. C. Fultz, Phys. Lett. **6**, 213 (1963).
[21] A. Veyssière, H. Beil, R. Bergère, P. Carlos, A. Leprêtre, and A. De Miniac, Nucl. Phys. **A227**, 513 (1974).
[22] A. J. F. Siegert, Phys. Rev. **52**, 787 (1937).
[23] K. Kino, T. Saito, Y. Suga, M. Oikawa, T. Nakagawa, T. Tohei, K. Abe, and H. Ueno, Phys. Rev. C **65**, 024604 (2002).
[24] S. Kamerdzhiev, J. Speth, and G. Tertychny, Nucl. Phys. **A624**, 328 (1997).
[25] R. Pitthan, F. R. Buskirk, J. N. Dyer, E. E. Hunter, and G. Pozinsky, Phys. Rev. C **19**, 299 (1979).
[26] G. O. Bolme, L. S. Cardman, R. Doerfler, L. J. Koester, Jr., B. L. Miller, C. N. Papanicolas, H. Rothhaas, and S. E. Williamson, Phys. Rev. Lett. **61**, 1081 (1988).